

Many-body physics of a quantum fluid of exciton-polaritons in a semiconductor microcavity

Iacopo Carusotto¹, Michiel Wouters^{1,2}, and Cristiano Ciuti³

¹ BEC-CNR-INFN and Università di Trento, I-38050 Povo, Italy

² TFVS, Universiteit Antwerpen, 2610 Antwerpen, Belgium

³ Laboratoire Pierre Aigrain, Ecole Normale Supérieure,
24, rue Lhomond, 75005 Paris, France

Some recent results concerning nonlinear optics in semiconductor microcavities are reviewed from the point of view of the many-body physics of an interacting photon gas. Analogies with systems of cold atoms at thermal equilibrium are drawn, and the peculiar behaviours due to the non-equilibrium regime pointed out. The richness of the predicted behaviours shows the potentialities of optical systems for the study of the physics of quantum fluids.

PACS numbers: 71.36.+c, 03.75.Kk, 42.25.Kb

1. INTRODUCTION

So far, the domain of nonlinear optics has remained quite distinct from the one of quantum fluids, and the concept that light propagating in a nonlinear optical medium consists of a gas of photons interacting via the medium nonlinearity has not been fully exploited yet. Nonlinear optical effects are generally observed using laser beams containing a huge number of coherent photons as light sources: the photon gas is therefore Bose condensed in a single, macroscopically occupied, mode. Maxwell equations of classical electromagnetism supplemented by a nonlinear polarization term are in fact the optical counterpart of the Gross-Pitaevskii equation for the \mathbf{C} -number matter field of an atomic condensate. Diluteness of the photon gas is ensured by the small value of the nonlinearity of most optical media.

In the present paper, we give a brief review of some among the most recent progress in the nonlinear optical properties of a semiconductor microcavity system¹ which appears as most suited for studying the many-body behaviour of a quantum fluid of light. Our attention will be focussed on as-

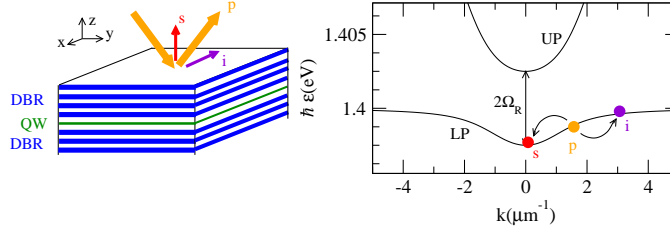


Fig. 1. Left panel: sketch of the microcavity structure and of the beams involved in the OPO process. Right panel: linear regime polaritonic dispersion and scheme of the OPO process.

pects of nonlinear optics that have a counterpart in quantum fluids, namely superfluidity², spontaneous symmetry breaking, and the Goldstone mode^{3,4}. In particular, we shall see how the non-equilibrium nature of the photon gas makes its behaviour much richer than the one of equilibrium Bose systems.

2. THE PHYSICAL SYSTEM

The physical system we consider¹ is sketched in Fig.1a. Light is confined in the cavity plane by a pair of planar Distributed Bragg Reflectors (DBR), formed by a stack of alternating $\lambda/4$ layer of different materials, e.g. AlAs and GaAs. The active material consists of a thin layer of a smaller gap material, e.g. InGaAs, present in the cavity layer: the Coulomb interaction between carriers results in a sharp optical line corresponding to the creation of a hydrogen-like electron-hole pair called exciton. If the excitonic transition is close to resonance to the cavity mode and the exciton-photon coupling Ω_R exceeds the excitonic and photonic linewidths $\gamma_{X,C}$, the eigenmodes of the system are *exciton-polaritons*, i.e. linear superpositions of cavity photon and quantum well exciton. This regime is conventionally called the *strong coupling* regime. In the low-density limit, polaritons satisfy Bose statistics. A simple description of the system is provided by the following second quantized Hamiltonian^{2,5}:

$$\begin{aligned}
 H &= \int d\mathbf{x} \sum_{ij=\{X,C\}} \hat{\Psi}_i^\dagger(\mathbf{x}) \mathbf{h}_{ij}^0 \hat{\Psi}_j(\mathbf{x}) + \frac{\hbar g}{2} \int d\mathbf{x} \hat{\Psi}_X^\dagger(\mathbf{x}) \hat{\Psi}_X^\dagger(\mathbf{x}) \hat{\Psi}_X(\mathbf{x}) \hat{\Psi}_X(\mathbf{x}) + \\
 &+ \int d\mathbf{x} \hbar \left(F_p(\mathbf{x}, t) \hat{\Psi}_C^\dagger(\mathbf{x}) + F_p^*(\mathbf{x}, t) \hat{\Psi}_C(\mathbf{x}) \right) + H_{\text{bath}}.
 \end{aligned} \tag{1}$$

The (bosonic) quantum field operators $\Psi_{C,X}(\mathbf{x})$ describing the cavity-photon C and the exciton X fields are defined in the 2D cavity plane. The single-

The quantum fluid of polaritons in semiconductor microcavities

particle Hamiltonian \mathbf{h}^0

$$\mathbf{h}^0 = \hbar \begin{pmatrix} \omega_X(-i\nabla) + V_X(\mathbf{x}) & \Omega_R \\ \Omega_R & \omega_C(-i\nabla) + V_C(\mathbf{x}) \end{pmatrix}, \quad (2)$$

involves the cavity-photon and exciton dispersions $\omega_{C,X}(\mathbf{k})$, and the electric-dipole exciton-photon coupling Ω_R . In the absence of confining potential $V_{C,X}(\mathbf{x}) = 0$, the eigenmodes of \mathbf{h}^0 correspond to the two polariton branches, the lower (LP) and the upper (UP) polariton. Their dispersion is plotted in Fig.1b. The excitonic content of the polariton is responsible for their binary interactions, which provide the optical nonlinearity of the system. The possibility of applying a spatial confinement potential $V_{C,X}(\mathbf{x})$ to polaritons by suitably nanostructuring the cavity has been recently demonstrated e.g. in Ref.6, which opens the way to polariton optics applications⁷.

All the terms in (1) mentioned so far have analogs in the second-quantized formulation of ultra-cold atom system. New physics arises from the last two terms, which respectively describe injection of polaritons into the cavity by a coherent light beam incident onto the front mirror, and their dissipation into the bath of other modes: $F_p(x, t)$ is proportional to the incident field amplitude. The main decay channel for the photon mode corresponds to the emission of radiation through the non-perfectly reflecting mirrors, while many different decay channels are available for the exciton mode, e.g. scattering on phonons, non-radiative exciton recombination at defects, excitation induced decoherence, etc.

3. HOW TO CREATE AND OBSERVE A POLARITON GAS

Creation, control and diagnostics of the polariton gas in the microcavity are generally performed by optical means through the cavity mirrors. This provides a clear advantage over most other quantum fluids, as optical injection of polaritons combines experimental simplicity with a wide flexibility. A variety of flow configurations can be generated by driving the cavity with a laser field with the suitable spatial and temporal profile $F_p(\mathbf{x}, t)$. Homogeneous and stationary flow along the cavity plane are obtained using a tilted pump beam of in-plane wavevector \mathbf{k}_p . More complex configurations showing e.g. vortical flow patterns are obtained using Laguerre-Gauss shaped pump beams⁸. It is interesting to stress the fact that polaritons are automatically created in the cavity in a coherent state; this state satisfying the Penrose-Onsager criterion^{9,10}, it can be seen as a (non-equilibrium) Bose condensate of polaritons.

The diagnostics of the polariton gas can be performed by optical means too, by measuring the light emitted by the cavity. Once direct reflection of

the pump laser is eliminated, the (operator-valued) electric field amplitude of the emitted light from the cavity is in fact proportional to the photonic component of the quantum polariton field¹¹. All correlation functions of the in-cavity polariton field are therefore directly translated into the corresponding ones of the extra-cavity emitted radiation, which are easily measured by means of standard optical interferometric techniques¹².

The first example of many-body property of the polariton gas to be studied has been superfluidity. A generalized Gross-Pitaevskii equation has been written²:

$$i \frac{d}{dt} \begin{pmatrix} \psi_X \\ \psi_C \end{pmatrix} = \left[\mathbf{h}^0 + \begin{pmatrix} g|\psi_X|^2 - i\gamma_X & 0 \\ 0 & -i\gamma_C \end{pmatrix} \right] \begin{pmatrix} \psi_X \\ \psi_C \end{pmatrix} + \begin{pmatrix} 0 \\ F_p \end{pmatrix} \quad (3)$$

and used to derive a non-equilibrium formulation² of the Landau criterion^{9,10} for superfluidity as a function of the pump beam intensity, frequency, and wavevector. When a very dilute polariton gas flowing along the cavity plane scatters on the sample imperfections, the typical ring-shaped profile of resonant Rayleigh scattering appears in the far-field emission. On the other hand, when the polariton gas becomes denser and the sound speed in it overcomes the flow velocity, the defect is no longer able to create excitations in the polariton fluid and the ring-shaped feature disappears from the far-field emission.

4. PARAMETRIC THRESHOLD AS A POLARITON BEC

Imposing the coherence from the outside is not the only way of obtaining a coherent polariton gas: several recent experiments have shown the spontaneous appearance of coherence under a sufficiently strong pumping^{13,14}. This *spontaneous coherence* is not imprinted from the outside, and often even appears in modes different from the ones which are optically pumped. In this respect, the system mostly resembles a laser above threshold, with the important difference that a continuum of modes available to the emission, so that the field is not frozen in a cavity mode, but has non-trivial spatial dynamics along the cavity plane. Although we will refer here to the specific example (Fig.1) of parametric oscillation^{5,13}, for which a complete and microscopic theoretical description is available¹¹, our conceptual framework can be extended to any other scheme showing spontaneous coherence^{14,15}. Pump polaritons are injected at \mathbf{k}_p and then converted into a pair of signal and idler ones at $\mathbf{k}_{s,i} \neq \mathbf{k}_p$ by the excitonic nonlinearity. Above a certain threshold, the emission at $\mathbf{k}_{s,i}$ goes from thermal to coherent as a consequence of the spontaneous breaking of a $U(1)$ signal/idler phase symmetry: the phase of the signal/idler emissions become coherent over long distances.

The quantum fluid of polaritons in semiconductor microcavities

According to the Penrose-Onsager criterion of Bose condensation¹⁰, one can therefore speak of a non-equilibrium Bose condensate.

This has been observed in Wigner-Quantum Monte Carlo simulations of the polariton field¹¹. The behaviour of the first- and second-order coherence functions of the signal emission results in the threshold region qualitatively identical to the one of a Bose gas at equilibrium in the vicinity of the Bose-Einstein condensation point. While approaching the critical point from below, the first-order coherence length increases, becomes macroscopic, and finally diverges at criticality. Above threshold, coherence extends across the whole sample. On the other hand, the second-order coherence function below threshold shows the typical Hanbury-Brown and Twiss (HBT) bosonic bunching upto distances of the order of the coherence length, and then goes back to 1. Above threshold, it is instead flat and equal to 1.

First experimental observations of these facts have been recently reported¹²: the long-distance coherence of the signal emission is inferred from the interference fringes that are obtained when light extracted at two distant points is made to beat. The monomode nature of the intensity noise of the signal emission above the threshold has been also established, which has ruled out the occurrence of effects of HBT type.

5. NEW FEATURES DUE TO NON-EQUILIBRIUM

Despite the many similarities, fundamental differences can arise because of the non-equilibrium nature of the system under investigation. Standard techniques of equilibrium statistical mechanics such as the Boltzmann law $p \propto \exp(-E/k_B T)$ can not be applied, and the stationary state of the polariton fluid is determined by a dynamical balance between driving (i.e. injection) and dissipation (i.e. losses). From this respect, the long-distance spatial coherence of the signal emission is an optical analog of the regular periodic arrangement of Bénard cells in heat convection¹⁶.

The *Goldstone mode* due to the spontaneously broken $U(1)$ symmetry is not a propagating sound-like mode, but rather a diffusive one³. This effect can be experimentally observed by probing the elementary excitations around the parametrically oscillating state with an additional laser beam. Pioneering luminescence experiments in this direction have been reported¹⁷.

At equilibrium, free-energy minimization arguments force the BEC to form in the lowest-energy state. Far from equilibrium, this constraint is lifted, and techniques mutuated from pattern formation can be used¹⁸ to determine the shape of the condensate mode as a function of the geometry and the pump frequency.

I. Carusotto, M. Wouters, and C. Ciuti

The spatial decay of coherence in non-equilibrium 1D systems¹⁹ is exponential even in the absence of thermal effects, with a coherence length ℓ_c inversely proportional to the damping rate γ and to the second derivative of the *imaginary* part of the *Goldstone mode* dispersion. This, in contrast to the equilibrium case where ℓ_c is inversely proportional to the temperature T and to the second derivative of the *real* part of the *free boson* dispersion⁴.

ACKNOWLEDGMENTS

M.W. acknowledges financial support from the FWO-Vlaanderen in the form of a “mandaat Postdoctoraal Onderzoeker”. LPA-ENS is a ”Unité Mixte de Recherche Associé au CNRS (UMR 8551) et aux Universités Paris 6 et 7”

REFERENCES

1. B. Deveaud (Ed.), *Physics of semiconductor microcavities*, Special issue of: *Phys. Stat. Sol. B* **242**, 2145-2356 (2005).
2. I. Carusotto and C. Ciuti, *Phys. Rev. Lett.* **93**, 166401 (2004)
3. M. Wouters and I. Carusotto, preprint *cond-mat/0606755*
4. M. Wouters and I. Carusotto, preprint *cond-mat/0512464*
5. C. Ciuti, P. Schwendimann, and A. Quattropani, *Semicond. Sci. Technol.* **18**, S279-S293 (2003) and references therein.
6. O. El Daif *et al.*, *Appl. Phys. Lett.* **88**, 061105 (2006)
7. A. Verger *et al.*, *Phys. Rev. B* **73**, 193306 (2006)
8. D. Rozas, Z. S. Sacks, and G. A. Swartlander, *Phys. Rev. Lett.* **79**, 3399 (1997).
9. L.P. Pitaevskii and S. Stringari, *Bose-Einstein Condensation*, Clarendon Press, Oxford (2003).
10. K. Huang, *Statistical Mechanics*, Wiley, New York, 1997.
11. I. Carusotto and C. Ciuti, *Phys. Rev. B* **72**, 125335 (2005)
12. A. Baas, *et al.*, *Phys. Rev. Lett.* **96**, 176401 (2006)
13. R. M. Stevenson *et al.*, *Phys. Rev. Lett.* **85**, 3680 (2000); R. Houdré *et al.*, *Phys. Rev. Lett.* **85**, 2793 (2000).
14. M. Richard, *et al.*, *Phys. Rev. B* **72**, 201301 (2005); H. Deng, *et al.*, *Science* **298**, 199 (2002); J. Kasprzak *et al.*, *Nature* **443**, 409 (2006)
15. D. Porras, *et al.*, *Phys. Rev. B* **66**, 85304 (2002); F. P. Laussy, *et al.*, *Phys. Rev. Lett.* **93**, 016402 (2004); D. Sarchi and V. Savona, preprint *cond-mat/0603106*; F. M. Marchetti, *et al.*, *Phys. Rev. Lett.* **96**, 066405 (2006).
16. M. C. Cross and P. C. Hohenberg, *Rev. Mod. Phys.* **65**, 851 (1993)
17. P. G. Savvidis, *et al.*, *Phys. Rev. B*, **64**, 075311 (2001)
18. M. Wouters and I. Carusotto, in preparation.
19. G. Dasbach, *et al.*, *Phys. Rev. B* **71**, 161308(R) (2005).